LLNL-JRNL-491452

LAWRENCE
LIVERMORE
NATIONAL
LABORATORY

Collisional Current Drive in Two Interpenetrating Plasma Jets

D. D. Ryutov, N. L. Kugland, H. S. Park, S. M. Pollaine, B. A. Remington, J. S. Ross

July 27, 2011

The Physics of plasmas

LLNL-JRNL-491452

Collisional current drive in two interpenetrating plasma jets

D.D. Ryutov, N.L. Kugland, H.-S. Park, S.M. Pollaine, B.A. Remington, J.S. Ross

Lawrence Livermore National Laboratory, Livermore, CA 94551, USA

Abstract

The magnetic field generation in two interpenetrating, weakly collisional plasma streams produced by intense lasers is considered. The generation mechanism is very similar to the neutral beam injection current drive in toroidal fusion devices, with the differences related to the absence of the initial magnetic field, short interaction time and different geometry. Spatial and temporal characteristics of the magnetic field produced in two counterstreaming jets are evaluated; it is shown that the magnetic field of order of 1T can be generated for modest jet parameters. Conditions under which this mechanism dominates that of the "Biermann battery" are discussed. Other settings where the mechanism of the collisional current drive can be important for the generation of seed magnetic fields include astrophysics and interiors of hohlraums.

Interaction of the laser-generated counter-streaming plasmas has recently drawn some attention in conjunction with experiments on collisionless shocks (e.g., [1-3]). A characteristic feature of these experiments is that, by their very design, the ion-ion mean-free paths are very large compared to the external spatial scale (the size of the zone where the streams are overlapping). On the other hand, the electron-ion collision times can still be quite short compared to the characteristic dynamic time, which is roughly the spatial scale divided by the ion velocity. The high electron collisionality is related to low electron temperatures: the electrons cool down by converting their initial thermal energy into the flow kinetic energy. The electron temperature in the interaction zone can be as small as 10^{-3} of the ion directed energy, especially if one deals with the plasma with the ion charge $Z>1$, where the ionization becomes an additional energy sink for the electrons.

In this brief communication we point out that the electron-ion collisions in the zone of the jets overlap can generate significant currents (and magnetic fields), provided the ion charge states in the two jets are different. Then, the condition of the zero total friction force acting on the essentially massless electron gas can be satisfied only in the presence of the net current. We will provide more specifics on this latter issue later in this note. Here we just mention that a very similar mechanism is used for the non-inductive current drive in toroidal fusion devices, where the ion streams are produced by tangential neutral beam injection [4, 5].

The overall geometry is schematically shown in Fig. 1. Shown are two jets at three instants of time, in the coordinate frame where the jet velocities are equal and opposite (this frame moves with respect to the lab frame with an average velocity of the jets, $(u_1+u_2)/2$). The origin $x=0$ is taken at the point where the jets first contact each other.

The instant of the first contact is taken as t=0. At t>0 there exists an overlap region (shaded). Jets are assumed axisymmetric, with the radial length-scale L, which is ~ 1 mm in the typical conditions of laser-based experiments [3]. As the characteristic time for the interaction process we take the time during which the length of the interaction zone becomes equal to the jet diameter:

$$\tau_{dyn} \equiv 2L/(u_1 - u_2) \tag{1}$$

We assume that u_1>0, u_2<0.

Table 1 contains parameters of fully ionized colliding jets that we consider below in numerical examples. The first case corresponds to collision of the carbon and beryllium jets. The second case corresponds to collision between the carbon and hydrogen jets (generation of the latter may be challenging as it may require the use of cryogenic targets).

Table 2 contains derived parameters for the two cases described in Table 1. One sees that for both cases of Table 1 the ion-ion scattering lengths are much larger than the size L of the interaction volume. On the other hand, the electron-electron mean-free path is quite short, signifying that the electron distribution is approximately Maxwellian.

The current drive mechanism is related to the friction force between two ion streams and the electron gas. We evaluate this force in the rest-frame of the electron gas (which does not necessarily coincide with the laboratory frame, for which the ion velocities in Table 1 are given). We will denote the velocity of this frame with respect to the lab frame by u, with u being positive if directed along the ion stream #1. For now we assume that both streams propagate along the same axis, which we denote by x.

To evaluate the effect of the current drive, we consider the momentum balance equation for the electron gas permeated by the ion streams. As the electron mass is small, one can neglect electron inertia. Then we have:

$$0 = -en_e E_x + n_e \nu_{ei}^{(1)} m(u_1 - u) + n_e \nu_{ei}^{(2)} m(u_2 - u) \tag{2}$$

where m_e is the electron mass, and $\nu_{ei}^{(1)}$ and $\nu_{ei}^{(2)}$ are the electron scattering frequencies on the ions of the stream 1 and 2, respectively. We evaluate them later in this note. We assume that the velocity of the first (second) jet is positive (negative): $u_1>0$, $u_2<0$. The electron density in the overlap zone is:

$$n_e = Z_1 n_{z1} + Z_2 n_{z2} \tag{3}$$

The origin of the electric field E_x in our problem is inductive: if the current is produced and the magnetic field appears, then the inductive electric field builds up. At the stage of the magnetic field growth it acts in the direction opposite to the "electromotive force" represented by the two last terms in Eq. (2). The electron-ion friction force is written under the assumption that the electron thermal velocity is significantly higher than the relative velocity of electrons and ions; this assumption holds by a significant margin for the parameters listed in Table 1.

The x-component of the current in our system is:

$$j_z = e(-n_e u + Z_1 n_{z1} u_1 + Z_2 n_{z2} u_2) \tag{4}$$

Combining equations (2)-(4), one finds:

$$\eta j_x = E_x + f_x \tag{5}$$

where η is the usual plasma resistivity (Cf. Ref. [6]):

$$\eta = \frac{m_e \nu_{ei}}{e^2 n_e} = \frac{m_e \nu_{ei}}{e^2 \left(n_1 Z_1 + n_2 Z_2\right)}; \quad \nu_{ei} = \nu_{ei}^{(1)} + \nu_{ei}^{(2)}, \tag{6}$$

and f_x is the electromotive force (having the dimension of the electric field) caused by the presence of two non-identical, oppositely directed ion streams:

$$f_x = -\eta e \frac{\left(u_1 - u_2\right)\left(Z_2 n_2 \nu_{ei}^{(1)} - Z_1 n_1 \nu_{ei}^{(2)}\right)}{\nu_{ei}^{(1)} + \nu_{ei}^{(2)}}. \tag{7}$$

One can present this expression in a remarkably simple form by noting that the electron-ion collision frequency depends on the ion density and charge as:

$$\nu_{ei}^{(1,2)} = D Z_{1,2}^2 n_{1,2}, \tag{8}$$

with the coefficient D being the same for both ion species. [There can be some small difference in the values of the Coulomb logarithms, but it is much smaller than the Z^2 dependence.] Substituting Eq. (8) in Eq. (7), one finds:

$$f_x = -\eta e \frac{\left(u_1 - u_2\right) Z_1 Z_2 n_1 n_2 \left(Z_1 - Z_2\right)}{n_1 Z_1^2 + n_2 Z_2^2} \tag{9}$$

One sees that, in order for this current drive mechanism to work, the ion charges in the two counter-streaming jets must be different. The electromotive force acts in the direction of the stream with a smaller charge. If one retains higher-order terms in the ratio $(u_{1,2}/v_{Te})^2$ in the expressions for the electron-ion drag forces entering into Eq. (2), one finds a non-zero drive for the ions in the same charge state. But for the examples of Tables 1 and 2 this correction is small.

An obvious generalization to the streams intersecting not in a head-on fashion is:

$$\boldsymbol{f} = -\eta e \frac{\left(\boldsymbol{u}_1 - \boldsymbol{u}_2\right) Z_1 Z_2 n_1 n_2 \left(Z_1 - Z_2\right)}{n_1 Z_1^2 + n_2 Z_2^2} \tag{10}$$

We will now evaluate the current and the magnetic field generated by this force. Using the Maxwell equations,

$$\nabla\times\boldsymbol{E}=-\frac{1}{c}\frac{\partial\boldsymbol{B}}{\partial t},\ \nabla\times\boldsymbol{B}=\frac{4\pi}{c}\boldsymbol{j}, \tag{11}$$

and writing Eq. (5) in a vectorial form, $\eta\boldsymbol{j}=\boldsymbol{E}+\boldsymbol{f}$, one finds:

$$\frac{\partial\boldsymbol{B}}{\partial t}=c\nabla\times\boldsymbol{f}-\nabla\times\left[D_M\nabla\times\boldsymbol{B}\right], \tag{12}$$

where D_M is the magnetic diffusivity, $D_M\equiv\eta c^2/4\pi$ .This equation is exactly the same as the one that would describe the well-known $\nabla n\times\nabla T_e$ current drive [7]; just the expression for the electromotive force is now different.

The magnetic field structure and magnitude depend on the temporal and spatial distribution of the electromotive force $\boldsymbol{f}$, as well on the magnetic diffusivity D_M. For the examples of Table1, the magnetic diffusion time,

$$\tau_M\equiv L^2/2D_M, \tag{13}$$

is long compared to the characteristic time of the jet-jet interaction (1), see Table 2.

The condition $\tau_M>>\tau_{dyn}$ allows one to drop the second term in the r.h.s. of Eq. (12). The magnetic field then is simply

$$\boldsymbol{B}=c\nabla\times\int_{-\infty}^{t}\boldsymbol{f}\,dt' \tag{14}$$

For the geometry of Fig. 1, where the system has an axis of symmetry, the electromotive force has only the x-component, depending on r and x; the magnetic field would then have only the azimuthal (φ) component: $B_\varphi=-c\partial/\partial r\left[\int_{-\infty}^{t}f_x\,dt'\right]$. The electromotive force is proportional to the particle density and gradually decreases to zero in the radial direction.

We evaluate the magnetic field for the model geometry of Fig. 1. Assuming the Gaussian distribution of the force, $f = f_0 \exp\left(-r^2 / L^2\right)$, where L is the radial length-scale, one sees that the magnetic field has a maximum at $r = L/\sqrt{2}$. At the midplane, x=0, this maximum is

$$B_{\max} = \sqrt{\frac{2}{e}}\frac{ct}{L} f_0 \tag{15}$$

where e=2.7318… . At other points along x, the field starts linearly growing with time since the moment when the overlap of flows occurs at this point. The general shape of the x-dependence of the magnetic field is then as shown at the bottom of Fig. 1. In a real situation, with the jets having smooth fronts, the breaks on the $B(x)$ dependence will, of course, be smoothed.

Taking as a characteristic time of the interaction the dynamic time (1), and using Eqs. (9) and (15), one finds the characteristic magnetic field B^* that can be generated by this mechanism:

$$B^* \equiv \frac{mc\nu_{ei}}{e}\frac{Z_1 Z_2 n_1 n_2 \left(Z_1 - Z_2\right)}{\left(n_1 Z_1^2 + n_2 Z_2^2\right)\left(n_1 Z_1 + n_2 Z_2\right)}. \tag{16}$$

(here and below, in all the semi-quantitative estimates we replace the factor $\sqrt{2/e} \approx 0.86$ by 1). By noting that eB^*/mc is electron cyclotron frequency ω_{Ce} corresponding to the field B^*, one can state that the characteristic magnetization parameter that is reached in the setting of Fig. 1 is

$$\frac{\omega_{Ce}}{\nu_{ei}} = \frac{Z_1 Z_2 n_1 n_2 \left(Z_1 - Z_2\right)}{\left(n_1 Z_1^2 + n_2 Z_2^2\right)\left(n_1 Z_1 + n_2 Z_2\right)} \tag{17}$$

For given charges Z_1 and Z_2, the strongest magnetization is reached at $n_2 / n_1 = \left(Z_1 / Z_2\right)^{3/2}$ and equals to $\left(Z_1 - Z_2\right)/\left(\sqrt{Z_1} + \sqrt{Z_2}\right)^2$. This can be quite close to 1.

We use the following numerical estimate for the electron-ion collision frequency (Cf. Ref. [6]):

$$\nu_{ei}(s^{-1}) \approx 2\times 10^{-5} \frac{\left(n_1(cm^{-3})Z_1^2 + n_2(cm^{-3})Z_2^2\right)}{\left[T_e(eV)\right]^{3/2}} \tag{18}$$

With that, the characteristic field B^* for the examples of Table 1 turns out to be ~ 1T (see the last column in Table 2). The actual value can be higher, as we used quite a short time τ_{dyn} as a characteristic interaction time (see Table 2). In the experiment the interaction time can be 2-3 times longer, leading to a corresponding increase of the magnetic field.

The self-generated magnetic field of this relatively high value may affect the plasma dynamics, in particular, by suppressing the electron thermal conductivity. It may be further enhanced by the plasma compression. Note that in addition to the regular magnetic fields produced by the aforementioned mechanism, there may also appear small-scale random magnetic fields generated by electromagnetic instabilities in counterstreaming flows (e.g., [8]). The regular magnetic field would be a background for these small-scale instabilities (if they are present in a particular setting).

Another mechanism of the spontaneous magnetic field generation that will act in parallel to that just described, is related to the non-collinearity of ∇n_e and ∇T_e [7] (it is sometimes called a "Biermann battery" in the astrophysical literature). Under the condition $\tau_M >> \tau_{dyn}$ it leads to generation of the magnetic field with the characteristic strength of $B^* \sim c\tau_{dyn}T_e / eL^2$. For the parameters of Tables 1 and 2, B^* is ~ 0.03 T. For higher electron temperatures, however, the $\nabla n \times \nabla T_e$ mechanism may become dominant: the collisional current drive scales as $T_e^{-3/2}$, whereas the $\nabla n_e \times \nabla T_e$ current drive scales as T_e. As an aside, one can mention that the $\nabla n_e \times \nabla T_e$ mechanism can also act at the front of a shock propagating at an angle to the density gradient, as seen in the experiment [9].

One can easily generalize this analysis to the case where there are more than two ion species involved. We present the result for the electromotive force for this more general case without derivation:

$$\boldsymbol{f} = \eta e \frac{\sum_{k,l} n_k n_l Z_k Z_l (Z_k - Z_l) \boldsymbol{u}_l}{\sum_k n_k Z_k^2} \tag{19}$$

This force becomes zero in case of the same charge states of all the ion species, as well in the case when all the ion species have the same velocity.

In summary: the collisional current drive considered in this note can easily lead to spontaneous generation of the magnetic field sufficient for the electron magnetization. It operates most effectively in the situations where the interpenetrating streams are made of ions with unequal *Z*. It can play a role in the astrophysical environment and as an effect that seeds the magnetic field in ICF experiments, in particular, in the intersecting plasma streams in hohlraums. The current drive is proportional to $T_e^{-3/2}$ and can operate at low electron temperatures.

This work was performed under the auspices of the U.S. Department of Energy by Lawrence Livermore National Laboratory under Contract DE-AC52-07NA27344.

TABLE 1
Sample parameters of the colliding jets

Case/Parameters	Jet 1				Jet 2			
	Z	A	n_z(cm^{-3})	u_z(cm/s)	Z	A	n_z(cm^{-3})	u_z(cm/s)
1	6	12	3×10^{18}	2×10^{8}	4	9	3×10^{18}	-2×10^{8}
2	6	12	3×10^{18}	2×10^{8}	1	1	5×10^{18}	-2×10^{8}

TABLE 2

Derived parameters for the examples of Table 1[a)]

Case/Parameters	λ_i, cm	λ_{ei}, cm	λ_{ee}, cm	ν_{ei}, s^{-1}	D_M cm^2/s	τ_M, s	τ_{dyn}, s	B*, T
1	75	0.8×10^{-3}	4×10^{-3}	1.1×10^{12}	10^{4}	5×10^{-6}	5×10^{-10}	1.1
2	200	1.2×10^{-3}	6×10^{-3}	0.7×10^{12}	1.1×10^{4}	4.5×10^{-6}	5×10^{-10}	0.7

[a)] In all cases, the electron temperature is assumed to be T_e=200 eV and the radial scale-length L=0.1 cm; λ_i is the scattering length of the lighter of the two ion components on the heavier one. The ratio $(u_{1,2}/v_{Te})^2$ is ~0.05 in both cases.

References

1. L. Romagnani, S.V. Bulanov, M. Borghesi, P. Audebert, J.C. Gauthier, K. Lowenbruck, A.J. Mackinnon, P. Patel, S. Glenzer, T. Toncian, O. Willi. “Observation of Collisionless Shocks in Laser-Plasma Experiments.” Phys. Rev. Lett., **101**, 025004 (2008).

2. Y. Kuramitsu, Y. Sakawa,T. Morita, C.D. Gregory, J.N. Waugh, S. Dono, H. Aoki, H. Tanji, M. Koenig, N. Woolsey, H. Takabe. “Time evolution of collisionless Socks in Counterstreaming Laser-Produced Plasmas.” Phys. Rev. Lett., **106**, 175002 (2011).

3. Hye-Sook Park, J. S. Ross, N. L. Kugland, et al. “Studying astrophysical collisionless shocks with counterstreaming plasmas from high power lasers,” ICHED Proceedings, Lisbon, May 2011; submitted to HEDP, August 2011.

4. T. Ohkawa, “New methods of driving plasma currents in fusion devices,” Nucl. Fusion, **10**, 185 (1970).

5. J. Wesson, “Tokamaks.” Oxford Science Publications, 1997. Sec. 3.13.

6. S.I. Braginski. “Transport processes in a plasma.” In: “Reviews of Plasma Physics” (M. A. Leontovich, Editor). Consultants Bureau, NY, 1965, p.205.

7. J.A. Stamper. “Review on spontaneous magnetic field in laser-produced plasmas – phenomena and measurements.” Laser and Particle Beams, **9,** 841 (1991).

8. E. S. Weibel. “Spontaneously growing transverse waves in a plasma due to an anisotropic velocity distribution.” Phys. Rev. Lett., **2**, 83, 1959.

9. G. Gregory, A. Ravasio, C.D. Murphy, et al. “Protogalactic magnetic field generation in laser-produced shock waves.” Submitted to Science, July 2011.

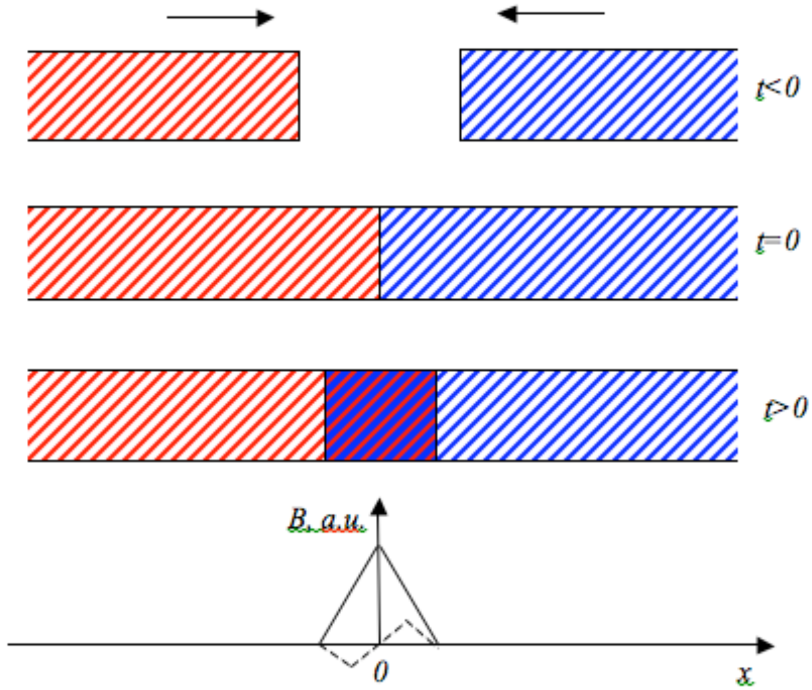

Fig. 1. Two colliding jets at different stages of their interaction. After jets overlap at $t>0$, the azimuthal magnetic field generation in the overlap region begins. The field distribution along the axis is an even function of x, with x measured from the midplane of the interaction zone. Note that the $\nabla n_e \times \nabla T_e$ mechanism would have produced the azimuthal field with an odd parity (schematically shown by the dashed line).